Chapter

Fiber Bragg Grating Sensors Integration in Fiber Optical Systems

Janis Braunfelds, Sandis Spolitis, Jurgis Porins and Vjaceslavs Bobrovs

Abstract

Fiber Bragg grating (FBG) sensors are a progressive passive optical components, and used for temperature, strain, water level, humidity, etc. monitoring. FBG sensors network can be integrated into existing optical fiber network infrastructure and realized structural health monitoring of roads, bridges, buildings, etc. In this chapter, the FBG sensor network integration in a single-channel and multi-channel spectrum sliced wavelength division multiplexed passive optical network (SS-WDM-PON) is presented and assessed. The operation of both the sensors and data transmission system, over a shared optical distribution network (ODN), is a challenging task and should be evaluated to provide stable, high-performance mixed systems in the future. Therefore, we have investigated the influence of FBG temperature sensors on 10 Gbit/s non-return-to-zero on–off keying (NRZ-OOK) modulated data channels optical transmission system. Results show that the crosstalk between both systems is negligible. The successful operation of both systems (with BER < 2×10^{-3} for communication system) can be achieved over ODN distances up to 40 km.

Keywords: fiber Bragg grating (FBG) sensors, sensor network, WDM-PON, SS-WDM-PON

1. Introduction

Optical fiber sensors are classified as intensity, phase, polarization, and wavelength modulated sensors based on their operating principles [1]. Fiber Bragg grating (FBG) sensors are wavelength modulated sensors or sensors which detect physical parameter (strain, temperature, and others) based on wavelength changes. Fiber Bragg grating (FBG) technology typically is used in optical filters, dispersion compensation modules, and sensors solutions. FBG sensors are passive optical components with high sensitivity and immune to electromagnetic interference and radio frequency interference, which can be integrated into existing optical fiber network infrastructure for structural health monitoring (SHM) applications [2–4]. FBG sensors can be used for roads, tunnels, bridges, rails, aircrafts SHM, as well as civil engineering, security, oil, and gas solutions monitoring [5]. With FBG sensors, it is possible to monitor various physical parameters such as temperature, strain, vibration, pressure, humidity, etc. [6–8].

It is necessary to analyze sensor influence on deployed and operating fiber optical communications systems data channels before FBG sensors integration in this fiber optical network infrastructure. Optical sensors signal interrogation (OSSI) units maximal monitoring distance between monitoring equipment and FBG sensors can be longer than 40 km.

First, in this paper optical sensor and single–channel 10 Gbit/s transmission system compatibility and co-operation were experimentally evaluated in the fiber-optical transmission system (FOTS) laboratory of Riga Technical University, Communication Technologies Research Center (RTU SSTIC), as described in Section 2 of this article.

Further, we have also demonstrated the collaboration with 32-channel spectrum-sliced wavelength-division-multiplexing passive optical network (SS-WDM PON) data channels and FBG sensor network in the simulation environment, as described in Section 3 of this article. Results showed that the optical transmission system with SS-WDM PON data and FBG sensor channels is an energy and cost-efficient solution, because its transmitter part is realized using a single amplified spontaneous emission (ASE) light source.

2. Evaluation of compatibility and co-operation on fiber-optic FBG sensor and single channel 10 Gbit/s NRZ-OOK transmission system

In this section, FBG temperature sensor integration and co-operation with operating fiber-optical transmission system are experimentally evaluated in the laboratory environment. The transmitter part of the experimental setup (see **Figure 1**) includes a broadband light source - ASE source, which is necessary to provide the operation of the deployed FBG sensor.

The measured output spectrum of the ASE light source is shown in **Figure 2**. The maximal peak power of around –10 dBm is located in wavelength bands of 1532–1534 and 1550–1560 nm. The high output power of the ASE light source and FBG sensor reflectivity is essential when monitoring distance (between the OSSI unit and FBG sensor) is long. Broad spectral band and fixed output power of the light source spectrum are crucial for multiplexing many sensors.

The output of the ASE light source is connected with an optical bandpass filter (OBPF). An OBPF (wavelength range: 1530 to 1610 nm (C&L Band), crosstalk >50 dB, bandwidth: 0.2 to 10.0 nm) is used to filtered spectral band for FBG temperature sensor. The spectral band is calculated based on FBG sensor defined operating

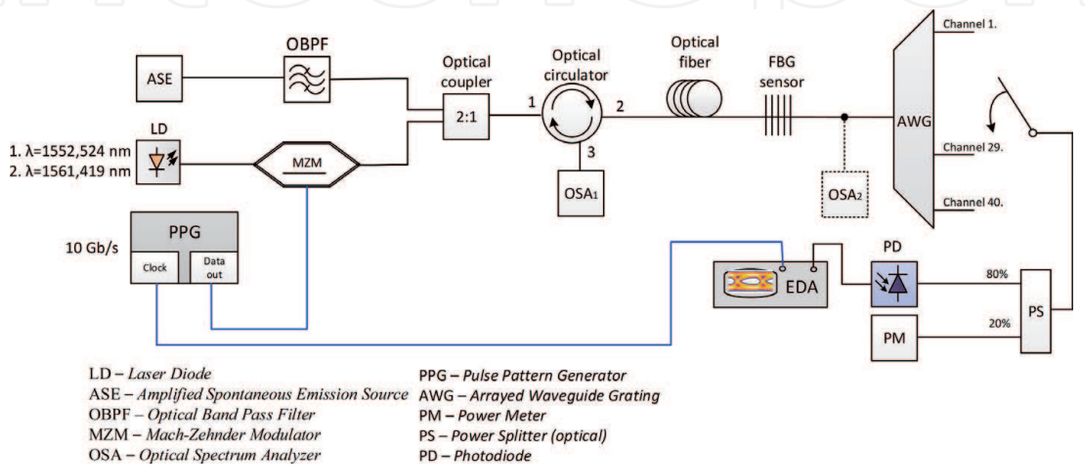

Figure 1.
Experimental setup of single–channel 10 Gbit/s transmission system with integrated optical FBG sensor.

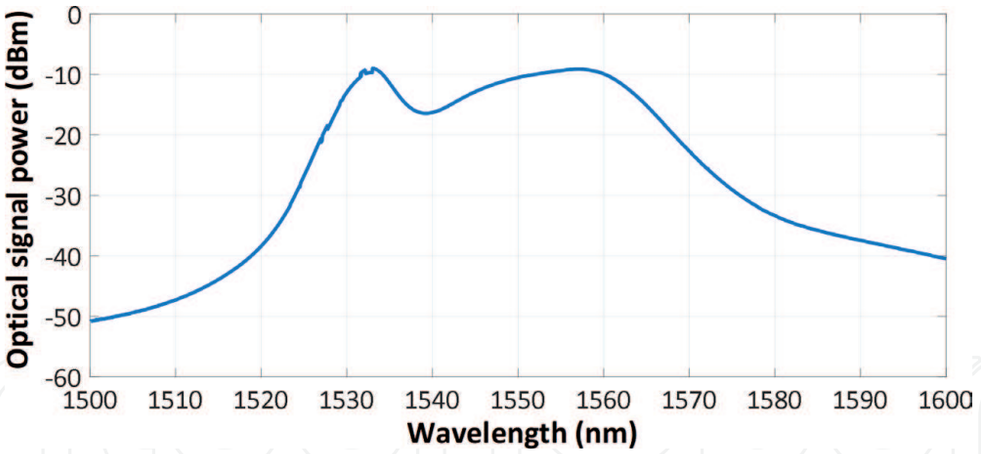

Figure 2.
Measured ASE output spectrum.

temperature band (−20 to +40°C). Temperature change by one degree causes a wavelength shift of 10.174 pm, taking into account the FBG reference temperature of 26°C ($\lambda_{ref} = 1565.191\,nm$). Wavelength shift depends on thermal-expansion coefficient and the thermal-optic coefficient of common single-mode fiber.

Central wavelength and frequency values for FBG temperature sensors are shown in **Table 1**. The wavelength band from 1565.05 to 1565.66 nm are set as a bandwidth of OBPF. The measured spectral curve of the OBPF passband is shown in **Figure 3**. The output of OBPF is connected to one of the optical coupler ports.

For the generation of FOTS data channel signal, the tunable laser diode (LD) with +9 (fiber length 20 km) and 12 dBm (fiber length 40 km) output power, 100 kHz linewidth, 50 dB sidemode suppression ratio (SMSR) is used. LD output is connected with Mach-Zehnder modulator (MZM) with polarization-maintaining PANDA type

Temperature	Wavelength [nm]	Frequency [THz]
−20 °C	1565.66	191.48
26°C	1565.19	191.54
40°C	1565.05	191.55

Table 1.
FBG temperature sensor central wavelength and frequency values.

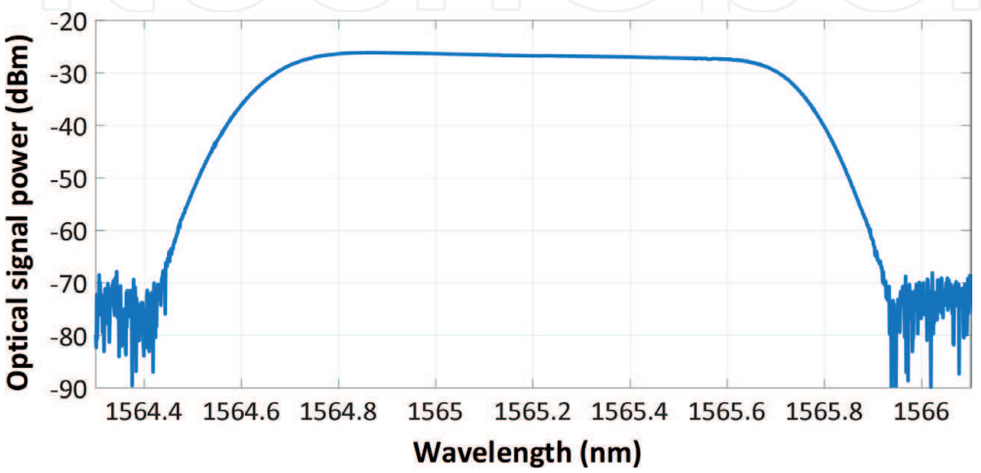

Figure 3.
Measured spectral curve of the OBPF filter passband.

fiber. Electrical data signals are generated by the pattern generator (PPG) (Anritsu, operating bitrate 10 Gbit/s, PRBS 2^{15}–1, signal purity –75 dBc/Hz). PPG data output and electrical RF input of the MZM is connected with proper RF cable. MZM optical output is connected with one of the optical power coupler (OPC) ports. OPC couples signals for FBG sensor and FOTS data channels.

OPC output is connected with the optical circulator (OC) port (1), necessary for separation of the sensor systems optical signal flows (transmitted and reflected). Please see the measured optical circulator insertion loss values in **Table 2**.

The optical circulator port (2) is connected with the optical fiber line and FBG sensor. 20 and 40 km long single-mode optical fiber (SMF-28) spools with insertion loss 4.3 and 8.3 dB are used in these experiments. The optical fiber output is connected with the FBG temperature sensor. FBG sensor structure and operation principle are shown in **Figure 4**.

FBG sensor technology is based on periodical reflection index changes in the fiber core [9–12]. FBG sensor reflects one part of the signal, but another part is transmitted further through the optical fiber. If the object's temperature changes, it shifts transmitted and reflected Bragg wavelength (λ_B), also known as signal central wavelength (see in **Figure 5**). OSA_1 and OSA_2 are used for the analysis of the FBG temperature sensor reflected and transmitted signals.

Bragg wavelength (λ_B) can be described by the following formula (1):

$$\lambda_B = 2 \cdot n_{eff} \cdot \wedge \tag{1}$$

Where:

Λ – grating period, nm;

n_{eff} – effective group reflection index;

λ_B – Bragg wavelength, nm [10].

FBG sensor temperature is calculated, based on the formula (2):

$$t = t_{ref} + \left(\frac{-\lambda_{ref} + \lambda_{mea}}{\Delta\lambda_{coe}} \right) \tag{2}$$

Where:

t_{ref} - reference temperature (defined in the sensor specification), °C

λ_{ref} – reference wavelength (defined in the sensor specification), nm

λ_{mea} - measured wavelength value, nm

$\Delta\lambda_{coe}$ – wavelength coefficient, describing wavelength shift, when temperature is changed per 1°C (defined in sensor specification), nm

Temperature sensor parameters used in experiments are listed in **Table 3**.

Direction	Measured insertion loss (dB)
1→2	2
2→3	1
1→3	60

Table 2.
The insertion loss of experimentally used optical circulator.

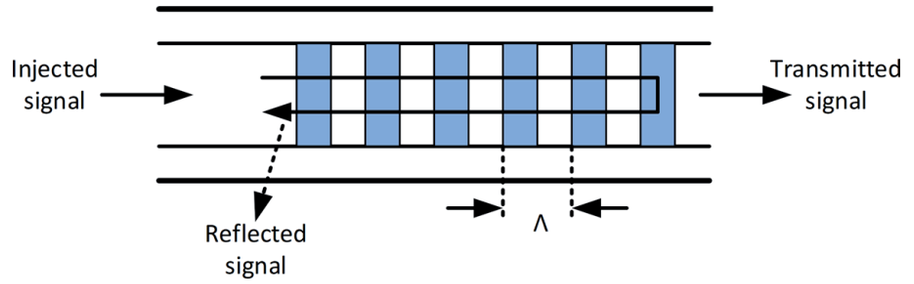

Figure 4.
FBG structure and operation principle.

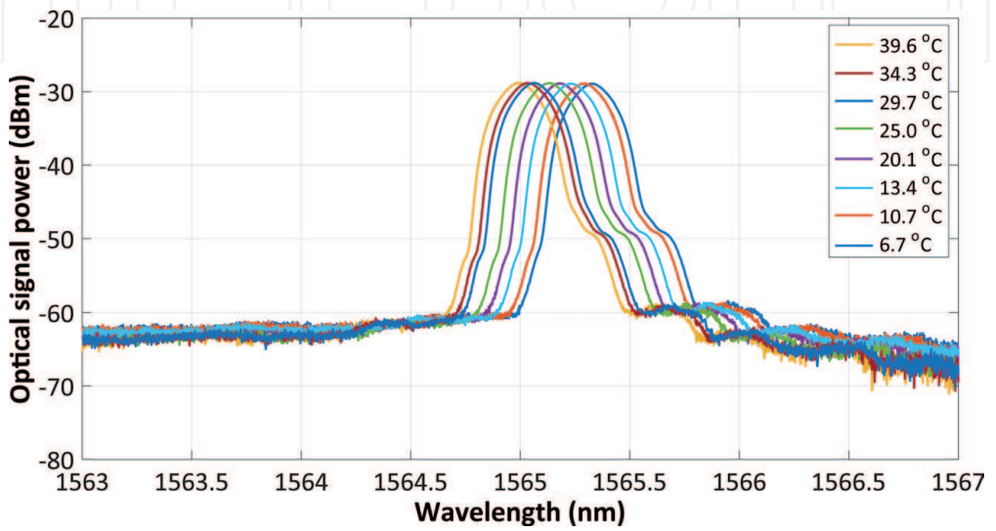

Figure 5.
Measured reflected FBG sensor signal spectrum at different temperatures.

FBG sensor parameter	Value
Reference temperature (t_{ref})	26°C
Reference wavelength (λ_{ref})	1565.191 nm
Wavelength coefficient ($\Delta\lambda_{coe}$)	10.174 pm
Sensor size	3 × 3 × 23 mm
Operation temperature band	−40 °C to +80°C

Table 3.
Parameters of experimentally used FBG temperature sensor.

As we can see in formula 2, and the measured graph (**Figure 6**), the temperature versus wavelength relationship has linear nature.

FBG output is connected with 40-channel (100 GHz channel spacing) arrayed waveguide grating (AWG) flat-top filter with operating wavelength band 1530.334–1561.419 nm (192–195.9 THz). The AWG is used to test the system with different spacing between data and sensor channels. The AWG (with 54 GHz 3-dB and 132 GHz 20-dB bandwidth) 29th and 40th channels are used in experiments, and its parameters are listed in **Table 4**.

AWG output is connected with optical power splitter (20:80%), where 20% are used for signal power monitoring, but 80% are transmitted to photo-diode (PD) (with sensitivity (1e-10 BER) = −20 dBm, operation wavelength range = 1280 nm–1580 nm and maximum output voltage = 350 mVp-p) that

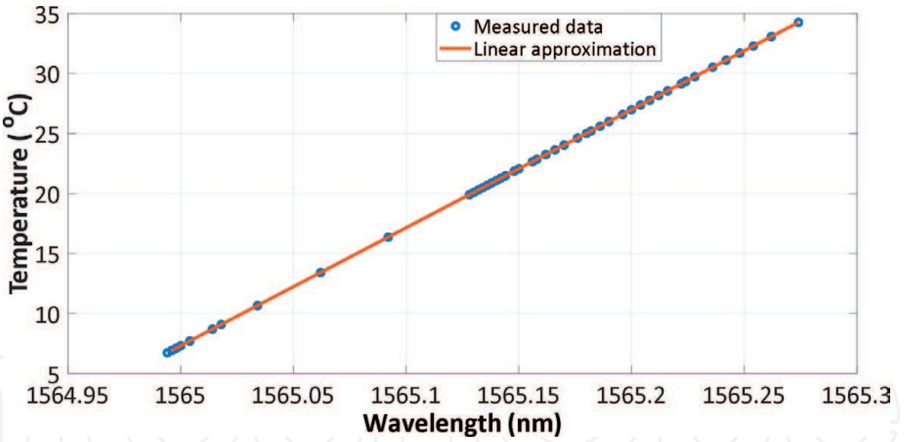

Figure 6.
Temperature versus wavelength relationship for experimentally used FBG temperature sensor.

No. of AWG Channel	Central wavelength [nm]	Frequency [THz]	Attenuation [dB]	
			min	max
29	1552.524	193.1	3.91	4.05
40	1561.419	192.0	4.28	4.41

Table 4.
AWG filter parameters 29th and 40th channel.

converts optical signal to electrical signal. PD output is fed through an RF cable to the eye diagram analyzer (EDA) for data signal quality analysis. For synchronization, the PPG clock signal is transmitted with RF cable to EDA.

Please see the measured FOTS data channel and FBG temperature sensor reflected spectrum in **Figures 7** and **8**, respectively. FBG temperature sensor reflected signal central wavelength is 1565.1279 nm, and the temperature (calculated with formula (2)) is 19.7°C.

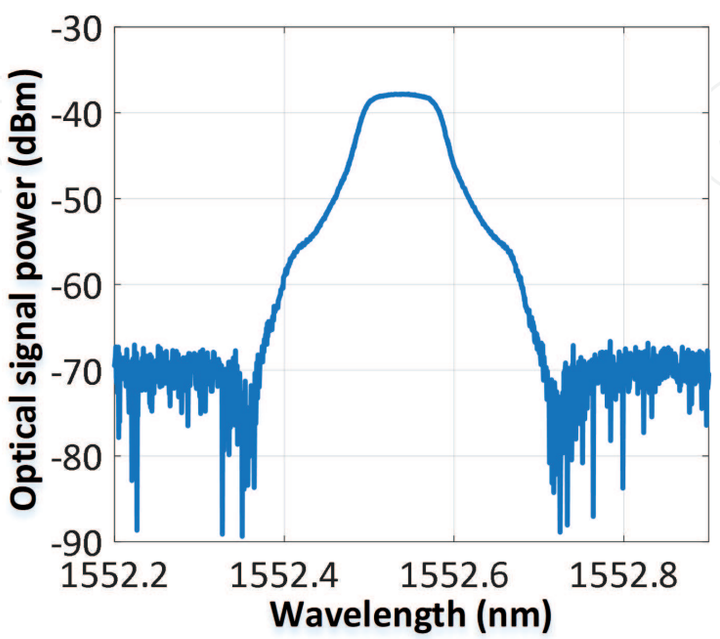

Figure 7.
Measured spectrum of transmission data channel.

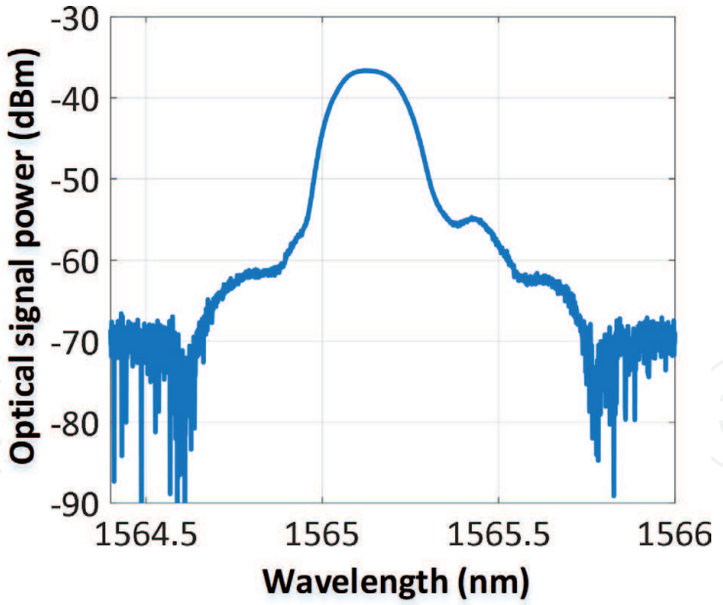

Figure 8.
Measured reflected spectrum of FBG temperature sensor.

Experimentally measured eye diagrams for NRZ-OOK modulated 10 Gbit/s FOTS (after 20 and 40 km long transmission) with and without integrated FBG temperature sensor are shown in **Figure 9**. As we can see in **Figure 9**, the data channel eye diagrams' quality is not degraded by the FBG sensor. Dispersion influence can be observed in eye diagrams (c, d) after 40 km signal transmission, which

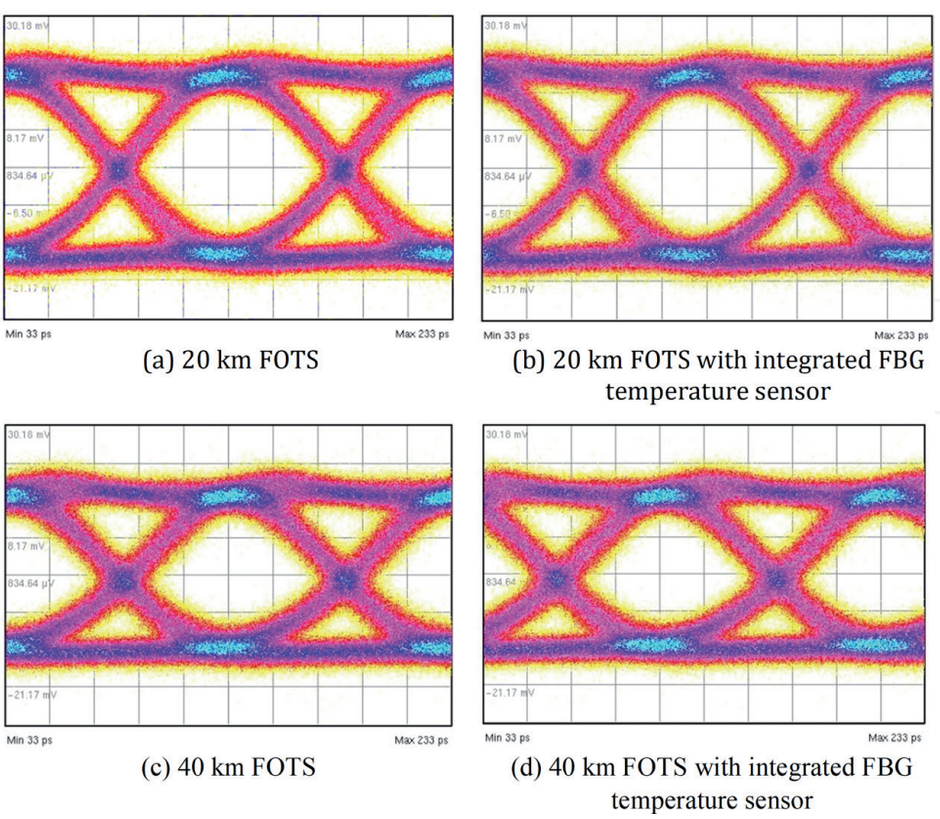

Figure 9.
Comparison of NRZ-OOK modulated 10 Gbit/s FOTS experimental eye diagrams. (a) 20 km FOTS. (b) 20 km FOTS with integrated FBG temperature sensor. (c) 40 km FOTS. (d) 40 km FOTS with integrated FBG temperature sensor.

can be prevented with chromatic dispersion (CD) compensation, such as dispersion compensation fiber (DCF).

3. Evaluation of combined FBG optical sensor network and 32-channel spectrum-sliced wavelength-division-multiplexing passive optical network system in simulation environment

The combined system's simulation setup with the FBG sensor network and SS-WDM PON data channels was developed within RSOFT OptSim software. The simulation setup is shown in **Figure 10**. In this system, only one shared broadband ASE light source is used. ASE spectrum was allocated in the spectral band between from 1533.47 to 1565.50 nm (in frequency band 191.5 THz and 195.5 THz). For SS-WDM PON systems, data transmission channels 1545.7 to 1558.2 nm.

(192.4 THz - 193.95 THz) spectrum was used, whereas 1537.4 to 1545.3 nm (194 THz - 195 THz) spectrum was used for optical FBG sensors network.

ASE light source is connected with an optical power splitter (50%:50%). One of the signal parts is transmitted to AWG MUX for data channel generation, but the second part to OBPF for sensor network. OBPF filtered spectral band from 1537.4 to 1545.3 nm (194 THz - 195 THz) for optical FBG sensor network. 32-channel AWG MUX is used in the setup, that filtered optical signal in the frequency band from 192.4 to 193.95 THz with 50-GHz channel spacing (according to ITU-T G.694.1 recommendation [13]) for 10 Gbit/s NRZ-OOK data channels transmitters. 3-dB bandwidth of each AWG's channel is set to 45 GHz. The data channels bitrate is set to 10 Gbit/s, considering 7% overhead for FEC encoding scheme application resulting in the total bitrate of 10.7 Gbit/s.

Each transmitter block consists of a semiconductor optical amplifier (SOA) to suppress intensity fluctuation noise coming from ASE and electro-absorption modulator (EAM) having immunity to signal polarization state (contrary to MZM). NRZ data signal is generated by data and NRZ component in simulation setup. 32 data channels are coupled with the AWG DEMUX block.

Additionally, DCF is used for dispersion pre-compensation. The transmission line dispersion coefficient is D = 16 ps/nm/km, but the total accumulated dispersion

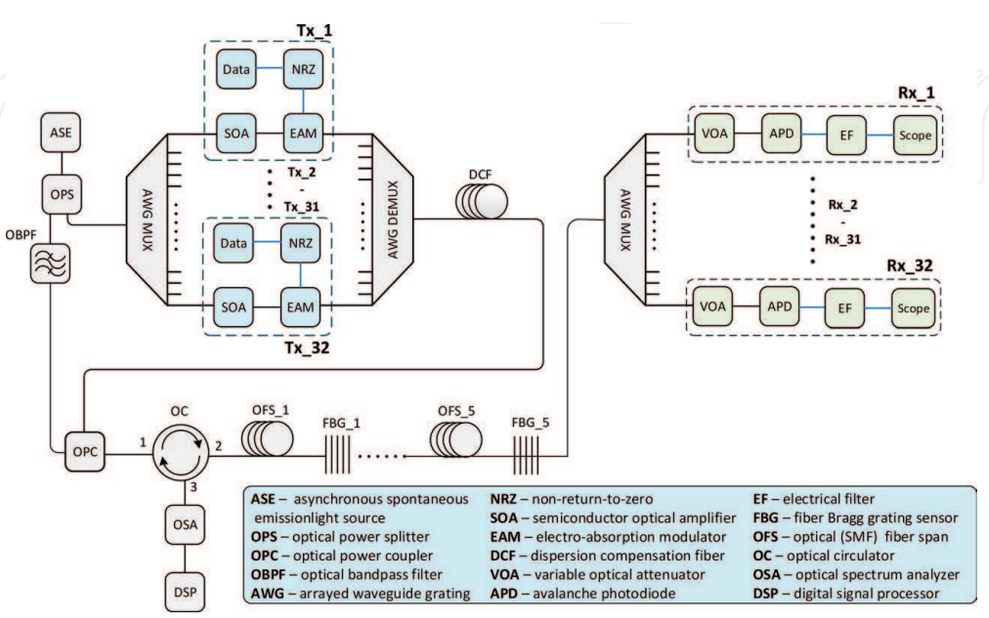

Figure 10.
Simulation setup of combined 32-channel 10 Gbit/s NRZ-OOK modulated SS-WDM-PON system with FBG temperature sensor network.

is 320 ps/nm. DCF fiber dispersion coefficient is −118.5 ps/nm/km, and the attenuation coefficient is α = 0.55 dB/km at 1550 nm reference wavelength. For total dispersion compensation, 2.7 km long DCF is used.

DCF fiber output is connected with one of the OPC input ports, but the second input port is connected with the OBPF output port. The coupled signal is transmitted to OC for separation of the sensor systems signal flows. OC port (2) is connected with 5 optical standard single-mode fiber (ITU-T G.652 recommendation [14]) spans (the length of each span is 4 km, insertion loss is 0.18 dB/km) and 5 FBG temperature sensors network (sensors central wavelength and frequency see in **Table 5**). The spectral band for operation in temperature band −40°C to +80°C (sensor parameters are listed in **Table 3**) is calculated for each sensor. FBG temperature sensor channel spacing is 200 GHz.

The FBG reflected signal from OC port (3) is transmitted to OSA for signal spectrum measurements. Central wavelength or frequency detection, and temperature value calculation are realized in a digital signal processor (DSP).

AWG MUX filtered signal of 32 channels is transmitted to the receiver block. Each receiver block consists of a variable optical attenuator (VOA), avalanche photodiode (APD), electrical filter (EF), and scope components. In this setup, VOA is used for SS-WDM-PON data channels' BER correlation diagram measurements. InGaAs APD (sensitivity set to −20 dBm at the reference BER of 10^{12}) converts optical signal to digital signal. Electrical Bessel low-pass filter 3-dB bandwidth is set to 6 GHz. The received signal quality is analyzed with the scope component, which measures signal eye diagrams and BER value.

FBG sensor's No.	Central wavelength (nm)	Central frequency (THz)
1	1544.53	194.1
2	1542.94	194.3
3	1541.35	194.5
4	1539.77	194.7
5	1538.19	194.9
Channel spacing	1.58	0.2

Table 5.
FBG temperature sensors central wavelength and frequency.

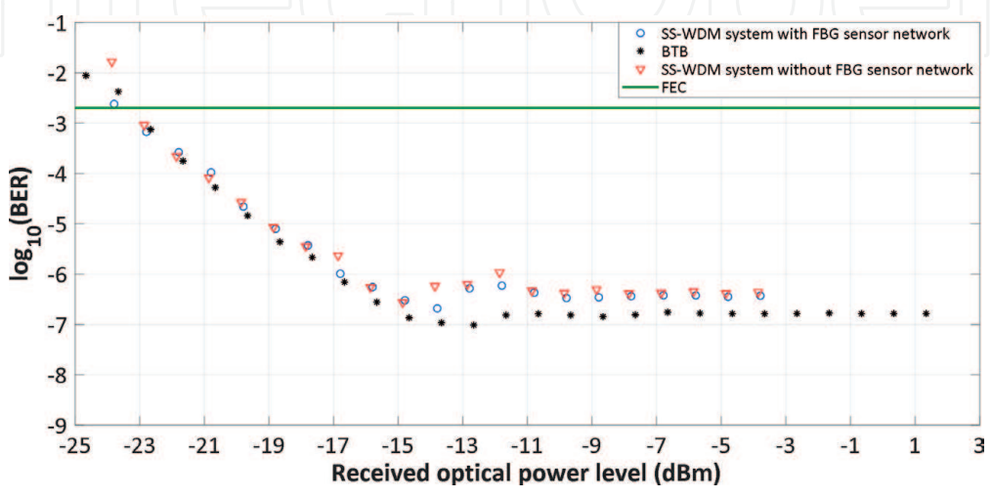

Figure 11.
BER versus received signal power (BER correlation diagrams) for SS-WDM PON system with and without an integrated FBG temperature sensing network.

The 3rd data channel provided the lowest performance of the combined system (SS-WDM-PON data channels and FBG sensor network). Measured BER versus received signal power, known as BER correlation diagram, for SS-WDM-PON system with and without integrated FBG temperature sensing network is shown in **Figure 11**. BER correlation diagram is measured for the worst-performing (in terms of BER) channel of the SS-WDM PON data transmission system.

As we can see in the measured BER versus received signal power (**Figure 11**) graph, the FBG influence on SS-WDM-PON transmission data channels is minimal. FOTS system power reserve is 19.5 dB at the pre-FEC BER level of 2×10^{-3} [15]. The measured BER value of back-to-back (BTB) systems with SS-WDM PON data channels and FBG sensor network is 3.72×10^{-7}, but for back-to-back (BTB) system 1.65×10^{-7}.

Based on the measured results, the calculated power penalty value (compared SS-WDM-PON system with and without integrated FBG temperature sensors network) is 0.5 dB at the pre-FEC BER level 2×10^{-3}.

4. Conclusion

In this research, we successfully demonstrated FBG temperature sensor integration in FOTS experimentally, but the combined system with FBG temperature sensor network and 32-channel spectrum-sliced wavelength-division-multiplexing passive optical network were realized in the simulation environment. The simulation model is based on one shared amplified spontaneous emission source. As shown in **Figures 9** and **11**, FBG sensors do not degrade data channel signal quality.

The measured BER value for the worst channel of a back-to-back (BTB) systems with SS-WDM-PON data channels and FBG sensor network is 3.72×10^{-7}, but for BTB system 1.65×10^{-7}. The FOTS systems power reserve is 19.5 dB at the pre-FEC BER level of 2×10^{-3}.

Acknowledgements

This work is supported by the European Regional Development Fund project No. 1.1.1.3/18/A/001, PVS 3912.6.2.

Conflict of interest

The authors declare no conflict of interest.

Data availability

The data used to support the findings of this study are available from the first author upon request.

Author details

Janis Braunfelds[1*], Sandis Spolitis[1], Jurgis Porins[2] and Vjaceslavs Bobrovs[2]

1 Riga Technical University, Communication Technologies Research Center, Riga, Latvia

2 Riga Technical University, Institute of Telecommunications, Riga, Latvia

*Address all correspondence to: janis.braunfelds@rtu.lv

References

[1] Taylor & Francis Group. Optical Fiber Sensors – Advances Techniques and Applications. CRC Press. 2015. pp. 545. DOI: 10.1201/b18074.

[2] Fidanboylu K., Efendioğlu H. S.b. Fiber optic sensors and their applications. In: 5th International Advanced Technologies Symposium (IATS'09); 13-15 May 2009; Karabuk, Turkey. pp. 7.

[3] Senkans U., Braunfelds J., Lyashuk I., Porins J., Spolitis S., Bobrovs V. "Research on FBG-Based Sensor Networks and Their Coexistence with Fiber Optical Transmission Systems". Hindawi. Journal of Sensors. 2019. 6459387.DOI: 10.1155/2019/6459387.

[4] Marcelo M. Werneck, Regina C. S. B. Allil, Bessie A. Ribeiro and Fábio V. B. de Nazaré. A guide to Fiber Bragg Grating Sensors. In: Christian Cuadrado-Laborde editors. Current Trends in Short- and Long-period Fiber Gratings. IntechOpen. 2013, pp. 24. DOI: DOI: 10.5772/54682.

[5] Braunfelds J., Senkans U., Lyashuk I., Porins J., Spolitis S., Bobrovs V. Unified Multi-channel Spectrum-sliced WDM-PON Transmission System with Embedded FBG Sensors Network. In: (2019) Progress in Electromagnetics Research Symposium; 17-20 June 2019; Rome, Italy; 2019. pp. 3327-3333.

[6] Senkans U., Braunfelds J., Lyashuk I., Porins J., Spolitis S., Haritonovs V., Bobrovs V. FBG sensors network embedded in spectrum-sliced WDM-PON transmission system operating on single shared broadband light source. In: 2019 Photonics and Electromagnetics Research Symposium - Fall, PIERS - Fall 2019 – Proceedings; 17-20 Dec. 2019; Xiamen, China; 2019. pp. 1632-1639.

[7] Campanella C.E., Cuccovillo A., Campanella C., Yurt A., Passaro V.M.N. "Fibre Bragg Grating based strain sensors: Review of technology and applications". MDPI. Sensors. 2018. 18 (9). 3115. DOI: 10.3390/s18093115.

[8] Laffont G., Cotillard R., Roussel N., Desmarchelier R., Rougeault S. "Temperature resistant fiber bragg gratings for on-line and structural health monitoring of the next-generation of nuclear reactors". MDPI. Sensors. 2018. 18 (6). 1791. DOI: 10.3390/s18061791.

[9] Laferrière J., Lietaert G., Taws R., Wolszczak S., "Reference Guide fo Fiber Optic Testing" JDSU. pp. 172. 2012.

[10] Qiao X., Shao Z., Bao W., Rong Q., "Fiber Bragg Grating Sensors for the Oil Industry". MDPI. Sensors. 2017. 17 (3). 429. DOI: 10.3390/s17030429.

[11] Zhang M., Xing Y., Zhang Z., Chen Q. "Design and Experiment of FBG-Based Icing Monitoring on Overhead Transmission Lines with an Improvement Trial for Windy Weather". MDPI. Sensors. vol. 14, no. 12. DOI: 10.3390/s141223954.

[12] Qiao X., Shao Z., Bao W., Rong Q. "Fiber Bragg Grating Sensors for the Oil Industry". MDPI. Sensors. 2017. 17. DOI: 10.3390/s17030429.

[13] ITU-T Recommendation G.694.1, Spectral grids for WDM applications: DWDM frequency grid, International Telecommunication Union, Telecommunication standardization sector of ITU, 2012, pp. 1-7.

[14] ITU-T Recommendation G.652, Characteristics of a single-mode optical fibre and cable, Telecommunication Union, Telecommunication standardization sector of ITU, 2017, pp. 1-28.

[15] Spolitis S., Bobrovs V., Parts R., Ivanovs G. Extended reach 32-channel dense spectrum-sliced optical access system, In: Progress in Electromagnetic Research Symposium (PIERS); 8-11 Aug. 2016. Shanghai, China; 2016. pp. 3764-3767.